JOURNAL OF MAGNETIC RESONANCE 67, 55–65 (1986)

Tip-Angle-Reduced T_1 Imaging

T. H. MARECI,*† W. SATTIN,*‡ AND K. N. SCOTT*†‡§

*Departments of *Radiology, †Physics, and ‡Nuclear Engineering Sciences, University of Florida, and §V.A. Medical Center, Gainesville, Florida 32610*

AND

AD BAX

Laboratory of Chemical Physics, National Institutes of Health, Bethesda, Maryland 20205

Received August 19, 1985

A new imaging technique is introduced which provides a series of stimulated echo images progressively weighted with T_1 relaxation with constant T_2 weighting. The series of T_1-weighted images is acquired during a single imaging sequence in a manner similar to a conventional T_2-weighted spin-echo imaging sequence. A 90° pulse creates transverse magnetization which is phase encoded and stored along the longitudinal axis by a 90° storage pulse. The image information is acquired by obtaining a series of stimulated echoes, each following a read pulse, which samples residual longitudinal magnetization not recovered to equilibrium. The tip angles of the read pulses are adjusted to given equal tip-angle weighting for each image. This is accomplished by making the tip angle of the first read pulse small and increasing the tip angle of each succeeding pulse, in a recursive manner, so that the last pulse in the series has a tip angle of 90°. This imaging method is dubbed tip-angle-reduced T_1 (TART) imaging.

INTRODUCTION

There are many methods of imaging the structure of an object of interest. One can rely on optical transmission or reflection of light in conventional microscopy, scattering of electrons by an object in electron microscopy, or X-ray transmission in plane or tomographic radiography. All these techniques use the transmission or reflection of incident radiation to create an image. In contrast, the technique of imaging with nuclear magnetic resonance is based on a fundamentally different process. A spatial dependence of the nuclear magnetic resonance frequency is created by imposing linear gradients on the main magnetic field. Hence the information contained in such an image is quite different from that obtained with the techniques mentioned above. The density of spins is represented by equilibrium magnetization and the local magnetic environment of the spins by the characteristic relaxation times.

The spatial resolution of nuclear magnetic resonance imaging is limited by the inherent signal strength, magnet inhomogeneities, and the ability to construct strong, linear field gradients which can respond in an appropriate time scale for an imaging technique. The resolving power of nuclear magnetic resonance imaging is sufficient

0022-2364/86 $3.00

by using a series of read pulses, each less than or equal to 90°, chosen to provide equal tip-angle weighting for each observed image in the series. The observed stimulated echo for each image is derived from the same storage and read mechanisms. Thus, the weighting due to relaxation is simplified while other echoes are suppressed with pulsed field gradients.

This approach is based on earlier work for the observation of either T_1 relaxation (*8*) or zero-quantum coherence (*9*) in a single pulse sequence. In both these cases, the spin system was initially prepared into the desired state and its time evolution observed with a series of read pulses small enough to only slightly perturb the evolving state. In the stimulated echo imaging technique described here, the first 90° pulse creates transverse magnetization which dephases in the inhomogeneous static field and is phase encoded with applied linear field gradients. The second 90° pulse splits the transverse magnetization into two equal parts. One portion remains as transverse magnetization forming an echo following the second 90° pulse. The other portion is stored as longitudinal magnetization which retains phase memory of the time evolution between the first two pulses. This stored longitudinal magnetization will relax to equilibrium with the usual time constant, T_1. If this stored magnetization is sampled with a read pulse before complete recovery to equilibrium has occurred, a stimulated echo is formed which retains phase encoded information and can be used to form an image. The residual longitudinal magnetization is reduced by the effect of the read pulse. For a series of read pulses, each less than or equal to 90°, the observed stimulated echo after each pulse can be used to form an image which has T_1 weighting dependent on the time interval between the 90° storage pulse and the specific read pulse which produces the echo of interest. A specific pulse sequence to produce a series of T_1-weighted stimulated echo images is shown in Fig. 1 with the pulse phase cycle given in Table 1. The choice of small tip-angle read pulses leads to a series of T_1-weighted images so this method has been dubbed, tip-angle reduced T_1 (TART) imaging.

The amount of transverse relaxation is the same for each image in the sequence of Fig. 1. Here it is assumed that the read gradient, g_x, is adjusted such that the echo due to magnet inhomogeneities and applied gradients occur at the same point in time. The storage pulse splits the magnetization into two equal parts; one portion forming the primary echo and the other stored as longitudinal magnetization. The primary echo following the 90° storage pulse will occur at a time, TE, after the slice selective 90° pulse which creates transverse magnetization. Ignoring diffusion and assuming ideal 90° pulses, the primary echo signal amplitude can be written as,

$$S_{1e} = \tfrac{1}{2}M_0 e^{-TE/T_2}, \qquad [1]$$

where M_0 is the equilibrium magnetization. The factor of one-half comes from the splitting of the transverse magnetization into two equal parts by the 90° storage pulse.

The residual longitudinal magnetization after a stimulated echo read pulse is reduced by a factor of the cosine of the read pulse tip angle. Hence the magnetization available to the next read pulse is reduced in magnitude. The tip-angle dependence of the signal intensity following the nth stimulated echo read pulse can be written as

$$S_n \sim \sin \alpha_n \left(\prod_{i=1}^{n-1} \cos \alpha_i\right), \qquad [2]$$

tip angles. A sequence of four read pulse tip angles satisfying Eq. [4] are shown in Table 2. These are the last four tip angles in any sequence and the series can be extended to any number of read pulses. Note that the observable signal intensity after each read pulse will decrease as the number of read pulses increases. The relative intensity of the observed signal in each image will be independent of the number of read pulses; however, the available signal-to-noise in each image will decrease as the number increases. Thus a practical limit will be reached dependent on the sensitivity of the imaging system.

Since the storage pulse occurs at TE/2, the stimulated echo occurs at a time TE/2 after the read pulse. Therefore the transverse relaxation weighting of each echo following a read pulse will be equal to that of the primary echo. Since the stored longitudinal magnetization is only affected by T_1 relaxation, the amount of T_1 relaxation for each stimulated echo is only dependent on the recovery time, RT, that has elapsed since the magnetization was initially stored along the longitudinal axis. The stimulated echo amplitude following the nth read pulse has relaxation weighting given by

$$S_n \sim e^{-\mathrm{TE}/T_2} e^{-\mathrm{RT}_n/T_1}. \qquad [5]$$

The effect of relaxation and tip-angle variation can be combined to give the stimulated echo amplitude following the nth read pulse,

$$S_n = \tfrac{1}{2} M_0 \sin \alpha_n \left(\prod_{i=1}^{n-1} \cos \alpha_i\right) e^{-\mathrm{TE}/T_2} e^{-\mathrm{RT}_n/T_1}. \qquad [6]$$

The reduced tip angles of the read pulses result in a reduction in available signal-to-noise ratio in the final images. This decrease in signal strength can be kept at a tolerable level by limiting the number of read pulses applied to create a T_1-weighted series of images. The four-pulse example of Table 2, results in a signal reduction for each stimulated echo image to 0.5 that of the primary echo image due to the reduced tip angle of the read pulses. Ignoring relaxation effects, this is an overall reduction in signal strength to 0.25 of the equivalent Carr–Purcell T_2-weighting series of images. The loss of signal strength does not increase dramatically as the number of read pulses increase because of the functional form of the tip-angle dependence. For example, the

TABLE 2

Final Four Tip Angles in a Series of n Read Pulses

Number of read pulse	Tip angle[a]
$n-3$	30°
$n-2$	35.3°
$n-1$	45°
n	90°

[a] Tip angles were calculated from Eq. [4] assuming the last read pulse tip angle equals 90°.

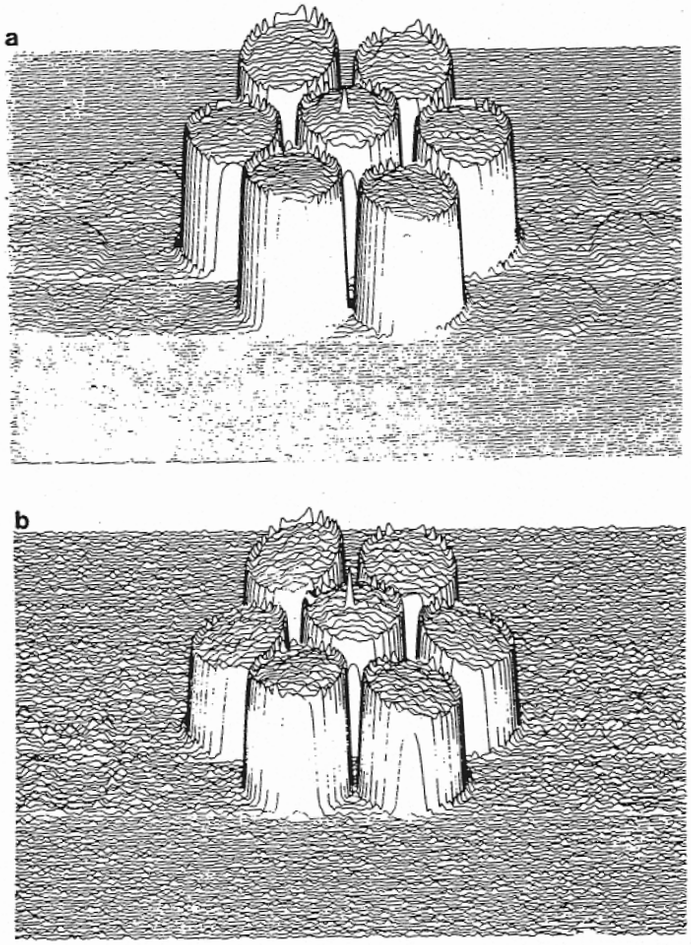

FIG. 2. Comparison of (a) conventional 90–180° spin-echo image and (b) TART 90–90° primary echo image.

this case y). The magnetic gradient system is oriented such that x is horizontal and y vertical. The baseline artifacts in the conventional spin-echo image of Fig. 2a are due to gradient instabilities in the phase-encoding gradient. The falloff of intensity in the phase-encoding direction for the TART primary echo image of Fig. 2b is of unknown origin but could be due to rf inhomogeneities. The same effect is not seen in the stimulated echo images following the read pulses in the TART sequence.

The T_1-weighted series of stimulated echo images for the TART sequence are shown in Fig. 3. The recovery time, RT, progresses in 50 ms steps increasing from 50 ms in Fig. 3a to 200 ms in Fig. 3d. By comparing the image of Fig. 2b with the first image in this T_1-weighted series, the expected 0.5 loss in signal-to-noise ratio is quite apparent. Qualitatively, the T_1-weighted series represents the available contrast difference due to variations in longitudinal relaxation rates.

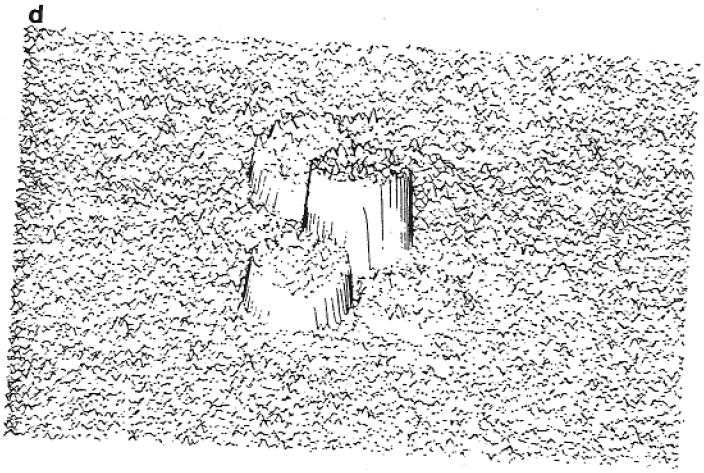

FIG. 3—*Continued*

To test the quantitative nature of the intensity variations in the TART image series, image intensity values were measured for all seven bottles in each image. These intensity values were determined by averaging pixels over a fixed-size region within the image boundaries of each bottle. The measured intensity values were used to determine the T_1 of each bottle by a two-parameter exponential curve fit to the four data points. The resulting values are shown in the second column of Table 3.

Each bottle was then removed from the phantom and placed in the center of the rf coil and the CSI system operated as a spectrometer without any applied imaging gradients or pulse shaping. The two pulse inversion–recovery T_1 sequence was applied to each bottle separately and eight data points were determined to define the recovery curve. The T_1 value of each bottle was determined by a three-parameter exponential curve fit and the values are reported in the fourth column of Table 3. There is quite good agreement between the two types of measurements indicating the TART sequence produces quantitative results at least in this experimental situation.

The central bottle contained a gel solution to effectively reduce its T_2. This would have indicated if an unexpected T_2 weighting was contributing to the T_1 weighting in the TART imaging series. The T_2 of this bottle was measured to be 58 ms as compared to the measured T_1 of approximately 230 ms. Since no appropriate reduction in the measured T_1 was observed, the TART sequence appears to have the expected relaxation weighting as described by Eq. [6].

CONCLUSIONS

The TART imaging experiment presented here represents a novel approach to T_1-weighted imaging which complements the conventional T_2-weighted spin-echo imaging sequence. The TART sequence has no rf pulses greater than 90°, so slice selection is more easily implemented with this sequence. Multislice, multiecho acquisition should be a straightforward generalization of the sequence in Fig. 1 without the attendant problems of slice selection with 180° pulses. Potentially, the TART sequence can provide a method of quantitative T_1 determination. However, potential problems due to misset tip angles and gradient pulse lengths need to be addressed before the limits

ACKNOWLEDGMENTS

These experiments were performed at General Electric NMR Instruments, Fremont, California, on the applications lab instrument. Special thanks go to Ralph Hurd for his help in performing these experiments and Ellory Schempp for his hospitality during our stay. This research was supported by grants from the National Institutes of Health (P41-RR-02278) and the Veterans Administration Medical Research Service.

REFERENCES

1. P. MANSFIELD AND P. G. MORRIS, *NMR Imaging in Biomedicine,* Academic Press, New York (1982), see Chapter 6.
2. T. L. JAMES AND A. R. MARGULIS (Eds.), "Biomedical Magnetic Resonance," Radiology Research and Education Foundation, San Francisco, 1984.
3. E. L. HAHN, *Phys. Rev.* **76,** 145 (1949).
4. H. Y. CARR AND E. M. PURCELL, *Phys. Rev.* **94,** 630 (1954).
5. S. MEIBOOM AND D. GILL, *Rev. Sci. Instru.* **29,** 688 (1958).
6. E. L. HAHN, *Phys. Rev.* **80,** 580 (1950).
7. W. SATTIN, T. H. MARECI, AND K. N. SCOTT, *J. Magn. Reson.* **64,** 177 (1985); *J. Magn. Reson.* **65,** 298 (1985); J. FRAHM, K. D. MERBOLDT, W. HÄNICKE, AND A. HAASE, *J. Magn. Reson.* **64,** 81 (1985); A. HAASE AND J. FRAHM, *J. Magn. Reson.* **64,** 94 (1985); K. D. MERBOLDT, W. HÄNICKE AND J. FRAHM, *J. Magn. Reson.* **64,** 479 (1985).
8. L. J. FRIEDMAN, Ph.D. Dissertation, Cornell University, Ithaca, N.Y., 1983.
9. A. BAX, T. MEHLKOPF, J. SMIDT, AND R. FREEMAN, *J. Magn. Reson.* **41,** 502 (1980).
10. P. MANSFIELD, *Magn. Reson. Med.* **1,** 370 (1984).